Desalination and Water Treatment
www.deswater.com
doi: 10.1080/19443994.2013.764352

51 (2013) 6038–6048
September

Taylor & Francis
Taylor & Francis Group

Citric acid modified wheat bran as a potential adsorbent for removal of Cu(II) and Malachite Green from aqueous solutions

Shamik Chowdhury*, Papita Das Saha

Department of Biotechnology, National Institute of Technology-Durgapur, Mahatma Gandhi Avenue, Durgapur 713 209, India
Tel. +91 9831387640; Fax: +91 3432547375; email: chowdhuryshamik@gmail.com

Received 18 September 2012; Accepted 2 January 2013

ABSTRACT

The contamination of water bodies by heavy metal ions and synthetic dye molecules from the wastewater streams of industries is a serious environmental problem. Wheat bran is currently an undervalued agricultural by-product. Therefore, the primary aim of this study was to develop a new economic wheat bran-based adsorbent with relatively high adsorption capacity for industrial wastewater treatment. Wheat bran was thermochemically modified with citric acid to prepare a biodegradable cationic adsorbent. The potential of using the prepared adsorbent for removal of Cu(II) and Malachite Green (MG) from aqueous solutions was then investigated using batch equilibrium tests. Operational parameters, such as solution pH, adsorbent dose, initial adsorbate concentration as well as temperature, greatly influenced the adsorption efficiency of the adsorbent. The Freundlich isotherm model showed excellent fit to the equilibrium data of Cu(II) while the Langmuir isotherm described best the adsorption data of MG. The sorption processes followed the pseudo-second-order rate kinetics. Thermodynamic study showed spontaneous and exothermic nature of the sorption processes. Results suggest that the use of citric acid modified wheat bran as adsorbent is a thoughtful and economic attempt for its needy utilization for treatment of industrial effluents.

Keywords: Adsorption; Citric acid-modified wheat bran; Cu(II); Malachite Green; Kinetics; Thermodynamics

1. Introduction

In today's modern society, the contamination of water bodies by heavy metal ions and synthetic dye molecules from the wastewater streams of industries represents a wide array of global environmental issues particularly due to their extreme toxicity towards aquatic life, human beings, and the environment [1,2]. Extensive research by scientists worldwide has led to the development of a wide range of treatment technologies (precipitation, ion-exchange, evaporation, oxidation, electroplating, membrane filtration, adsorption, photo-degradation, biodegradation, photocatalytic-degradation, destruction, irradiation, and ozonation) with varying levels of success. Of special interest, adsorption has been identified as the most efficient and economically viable sustainable technology for the removal of heavy metals and dyes from the wastewater streams of industries [3,4]. The importance and usefulness of adsorption in wastewater treatment is well established [3,4]. A huge number of low-cost adsorbents based on natural materials or agro-industrial wastes have been investigated intensively for removal

*Corresponding author.

of organic and inorganic pollutants from aqueous media [3–5].

Wheat is one of the world's four major cereal grains (wheat, maize, rice, and barley) and is also the most important source of calories and dietary proteins for humans [6]. Most of the grain used for human food is milled to remove the bran (pericarp) and germ, primarily to meet sensory expectations of consumers. Thus, a large amount of wheat bran is produced as by-product during the milling operation [7]. Millers often dispose of wheat bran because the cost of transportation is more than it's worth, and such waste also causes potential environmental concerns [8]. The chemical composition and chemical diversity of wheat bran, however, make it an interesting biomass for further applications. Major constituents in wheat bran are non-starch carbohydrates (~58%), starch (~19%) and crude protein (~18%), with non-starch carbohydrates being ~70% arabinoxylans, ~24% cellulose, and 6% β-(1,3)(1,4) glucan[9]. Arabinoxylans (a class of hemicellulose) consist of a backbone of β-(1→4)-linked D-xylopyranosyl residues substituted in various proportions withα-L-arabinofuranosyl units at O-2, O-3 and/or both O-2 and O-3 positions and 4-O-methyl-β-D-glucopyranosyl uronic acid residues at position O-2 [10]. Therefore, the primary objective of this study was to develop a new economic technique for wheat bran exploitation and utilization.

In the present study, wheat bran was thermochemically modified with citric acid to prepare a biodegradable cationic adsorbent. Citric acid is a low cost material used extensively in the food industry [11]. The citric acid modification of wheat bran involves two steps [12]. The first step involves formation of a reactive internal anhydride (5-member ring formation) between two adjacent carboxylic acid groups of the citric acid molecule, resulting in the loss of one molecule of water. In the second step, the anhydride reacts with the sugar hydroxyl groups to form an ester linkage between the two substrates and leaves two acid groups remaining on the citric acid molecule. The introduced free carboxyl groups of citric acid increase the net negative charge on the wheat bran fiber, thereby increasing its binding potential for cationic contaminants. The modification of wheat bran can be schematically expressed by the equation:

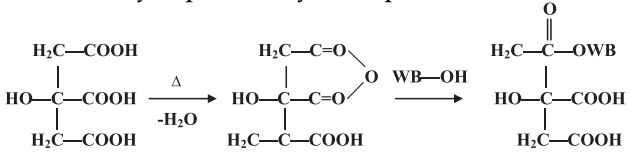

The potential of using the citric acid modified wheat bran (CMWB) as adsorbent for removal of metal ions (copper ion) and dye (Malachite Green, MG) from aqueous media was further tested employing a batch experimental set-up. The effect of parameters like solution pH, adsorbent dose, adsorbate concentration, and temperature was studied. Langmuir, Freundlich, and Dubinin–Radushkevich (D–R) models were used to describe the equilibrium data. The sorption mechanism was also evaluated in terms of kinetics and thermodynamics.

2. Materials and methods

2.1. Preparation and characterization of CMWB adsorbent

Wheat bran was obtained from a local wheat mill of Durgapur, West Bengal, India. It was washed thoroughly with distilled water to remove soil and dust. The wet bran was spread in a stainless steel tray and oven dried at 323 ± 1 K for 24 h. The dried wheat bran was then ground and sieved to retain the 20–40 mesh fractions for further modification.

The ground wheat bran was thermochemically modified with citric acid according to the procedure described by Vaughan et al. [13]. Ground wheat bran was mixed with 0.6 M citric acid at a ratio of 1:12 (bran/acid, w/v) and stirred for 30 min at room temperature. The acid bran slurries were then placed in a stainless steel tray and dried at 323 ± 1 K in a forced air oven for 24 h. Then, the thermochemical esterification between the acid and the bran was proceeded by raising the oven temperature to 393 ± 1 K for 90 min. The bran was then removed from the oven and allowed to cool. After cooling, the CMWB was washed with distilled water until the liquid did not turn turbid. The wet CMWB was then dried at 323 ± 1 K for 24 h and stored in a sterile, air-tight glass bottle for further use as an adsorbent.

In order to get insights on wheat bran morphology and its modification following the thermochemical treatment, both natural wheat bran (NWB) and CMWB were characterized by surface area and porosity analyzer, Fourier transform infrared (FTIR) spectroscopy, and scanning electron microscopy (SEM). The Brunauer, Emmett, and Teller (BET) surface area and pore size of NWB and CMWB were measured by a surface area and porosity analyzer (NOVA 2200, Quantachrome Corporation, USA). A gas mixture of 22.9 mol% nitrogen and 77.1 mol% helium was used for this purpose. FTIR spectrum of wheat bran before and after thermochemical modification was recorded with a FTIR spectrometer (Spectrum BX-II, PerkinElmer, USA). About 0.001 g of dry sample was mixed with 0.5 g of spectroscopic grade potassium bromide powder in an agate pestle and mortar. The powder

was then compressed into a thin KBr translucent disk under a pressure of 100 kg cm^{-2} for 8 min with the aid of a bench press. FTIR spectra were then recorded in the wave number range 4,000–1,000 cm^{-1} at 4 cm^{-1} spectral resolution. The surface structure of NWB and CMWB was analyzed by a SEM (S-3000N, Hitachi, Japan) at an electron acceleration voltage of 20 kV. Prior to scanning, the NWB and CMWB samples were mounted on a stainless steel stab with double stick tape and coated with a thin layer of gold in a high vacuum condition.

2.2. Preparation of Cu(II) and MG solutions

Cu(II) and MG stock solutions (500 mg L^{-1}) were prepared by dissolving accurately weighed quantity of $CuSO_4.5H_2O$ (analytical reagent grade) and $C_{23}H_{25}N_2Cl$ (analytical reagent grade) in double-distilled water, respectively. Experimental solutions of different concentration (20, 40, 50, 60, 80, 100 mg L^{-1}) were prepared by diluting the stock solution with suitable volume of double distilled water. The initial solution pH was adjusted with 0.1 M HCl and 0.1 M NaOH solutions using a digital pH meter (LI 127, ELICO, India) calibrated with standard buffer solutions.

2.3. Adsorption studies

Batch mode adsorption studies of Cu(II) and MG were carried out in 250-mL glass-stoppered Erlenmeyer flasks with 100 mL of working volume, with a concentration of 50 mg L^{-1}. A weighed amount (3 g) of adsorbent was added to the solution. The flasks were agitated at a constant speed of 150 rpm for 6 h in an incubator shaker (Innova 42, New Brunswick Scientific, Canada) at 303 ± 1 K. The influence of initial solution pH (2, 3, 4, 5, 6, 7, 8, 9, 10), adsorbent dose (0.5, 1, 2, 3, 4, 5 g), initial adsorbate concentration (20, 40, 60, 80, 100 mg L^{-1}), and temperature (293, 303, 313 K) were evaluated during the present study. Samples were collected from the flasks at predetermined time intervals for analyzing the residual adsorbate concentration in the solution. The residual amount of Cu(II) in each flask was determined according to the method described in paper [14]. The residual MG concentration was estimated by monitoring the change in absorbance values at maximum wavelength (λ_{max}) of 618 nm using a UV/VIS spectrophotometer (U-2800, Hitachi, Japan).

The amount of adsorbate adsorbed per unit adsorbent (mg adsorbate per g adsorbent) was calculated according to a mass balance on the adsorbate concentration using Eq. (1):

$$q_e = \frac{(C_i - C_e)V}{m} \quad (1)$$

The percent removal (%) was calculated using the following equation:

$$\text{Removal } (\%) = \frac{C_i - C_e}{C_i} \times 100 \quad (2)$$

In order to ensure the reproducibility of the results, all the adsorption experiments were performed in triplicate, and the average values were used in data analysis. Relative standard deviations were found to be within ± 3%. Linear regression analyses were used to determine slopes and intercepts of the linear plots and for statistical analyses of the data.

3. Results and discussion

3.1. Characterization of CMWB adsorbent

The specific surface area and pore size as estimated by the BET method were found to be 9.15 m^2 g^{-1} and 13.49 nm for NWB and 17.62 m^2 g^{-1} and 55.10 nm for CMWB, respectively. The surface area increased about two times after modification. The increase in the surface area of the wheat bran upon acid treatment followed by heat activation is attributed to the removal of water molecules both formed during acid activation and those inherently present as crystal water [15]. The pore size in CMWB is larger than that in NWB. The pores are large enough to allow the penetration of metal ions and dye molecules.

SEM micrographs of wheat bran before and after thermochemical treatment give further insight on wheat bran morphology and its modification during the treatment (Fig. 1). Wheat bran before treatment is characterized by irregular and porous surface. Thermochemical treatment increased the surface roughness, which indicates high surface area as already inferred from the BET analysis. In addition, distinct cracks and fissures could be a consequence of the preferential elimination of the cementing materials of the interfibrillar region during the treatment process.

The characteristic peaks of NWB and CMWB as revealed by FTIR analysis are shown in Table 1. In the spectrum of NWB, the peaks at 4,250 and 3,890 cm^{-1} represents N–H stretching, suggesting the presence of amino and amide functional groups. The broad band at around 3,340 cm^{-1} is due to the O–H stretching of the hydroxyl groups. The band at 1,632 cm^{-1} is attributed to carbonyl groups of aldehydes and ketones. Peaks at 1,460 and 1,375 cm^{-1} correspond to C–H

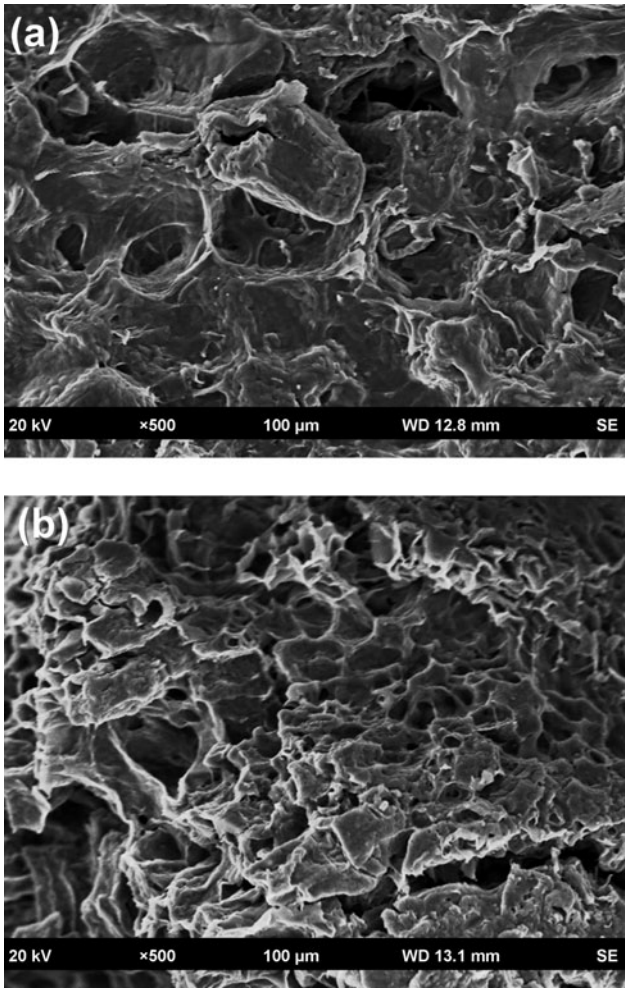

Fig. 1. SEM micrograph of (a) WB (b) CMWB.

Table 1
FTIR absorption peaks of NWB and CMWB

Wavenumber (cm^{-1})		Assignment
NWB	CMWB	
4,250, 3,890	3,960	N–H stretching of $–NH_2$ and –C(=O) NH_2 groups
3,340	3,255	O–H stretching
–	1,743	C=O stretching of –COOH
1,632	1,635	C=O stretching of R–CHO and RC (=O)R´
–	1,616	C=O stretching of –COOH
1,460	1,432	C–H bending
1,375	1,374	C–H bending
1,050	1,060	C–O–C stretching of carbohydrates

bending vibration. The band at 1,050 cm^{-1} is indicative of C–O–C stretching vibrations in carbohydrates. Following thermochemical treatment, two new peaks are observed at 1,743 and 1,616 cm^{-1}, respectively. The peak at 1,743 cm^{-1} can be attributed to un-ionized C=O stretching of carboxylic acid while the peak at 1,616 cm^{-1} is indicative of C=O stretching of carboxylic group with intermolecular hydrogen bond. These findings confirm the introduction of free carboxylic acid groups on the surface of the material.

Owing to the presence of new functional groups, increased surface area, and larger pore size, CMWB is expected to possess greater adsorption capacity than NWB.

3.2. Batch adsorption studies

3.2.1. Effect of pH

The solution pH is an important monitoring parameter governing an adsorption process. It not only influences the surface charge of the adsorbent but also the degree of ionization of the adsorbate species present in the solution. Therefore, in the present investigation, batch experiments as described above were carried out in the pH range 2–10 to evaluate the effect of pH on the adsorption efficiency of CMWB. It is to be noted that copper is present as free Cu(II) species along the whole acid pH range. Above pH 7.0, it starts to precipitate as $Cu(OH)_2$, and thus, no more "available" for adsorption. Hence, no further experiments were performed beyond pH 7.0 while studying the effect of pH on Cu(II) adsorption.

The results of the pH profile study are shown in Fig. 2(a). In both the systems, the percentage removal sharply increases with increase in pH. The removal efficiency increases when pH of the solution is raised above three and is maximum at pH 6 for Cu(II) adsorption. Maximum adsorption of MG is observed at pH 8. Quite similar tendency was reported for adsorption of Cu(II) by chestnut shell [16] and MG by treated ginger waste [17].

This observed trend of increase in percentage removal with increase in solution pH can be well explained by taking into consideration the overall charge on the adsorbent surface. FTIR analysis of CMWB showed that the adsorbent contains a variety of functional groups namely carboxyl, carbonyl, hydroxyl, amino, amido, etc. With the change in solution pH, the behavior of each of these functional groups changes. For example, carboxyl groups are protonated at highly acidic pHs (pH less than 3) and act as positively charged species and thus, can

attract negatively charged ions [18]. On increasing the pH, deprotonation (ionization) of these functional groups occur. They become negatively charged moieties and can attract positively charged ions. In general, at highly acidic pHs, binding of positively charged adsorbate ions is reduced due to electrostatic repulsions because of the positive nature of the adsorbent and the binding increases with the increase in pH, because the adsorbent becomes negatively charged.

3.2.2. Effect of adsorbent dose

Fig. 2(b) shows the adsorption profile of Cu(II) and MG vs. different adsorbent concentration in the range of 0.5–5.0 g. It is observed that the percentage removal of Cu(II) and MG increase with increasing adsorbent dose. The positive correlation between adsorbent dose and percentage removal can be related to increase in adsorbent surface area and availability of more adsorption sites [19]. Maximum percentage removal (96.35%-Cu(II); 92.68%-MG) is observed at around 3.0 g and further increase in adsorbent dose does not significantly change the adsorption yield which is mainly due to the binding of almost all adsorbate ions to the adsorbent surface and the establishment of equilibrium between the adsorbate on the adsorbent and in the solution. Therefore, in the following experiments, the adsorbent dose was fixed at 3.0 g. Similar behavior for the effect of adsorbent dose was observed and discussed in the literature for the adsorption process of Cu(II) onto *Capsicum annuum* seeds [20] and MG onto sea shells [1].

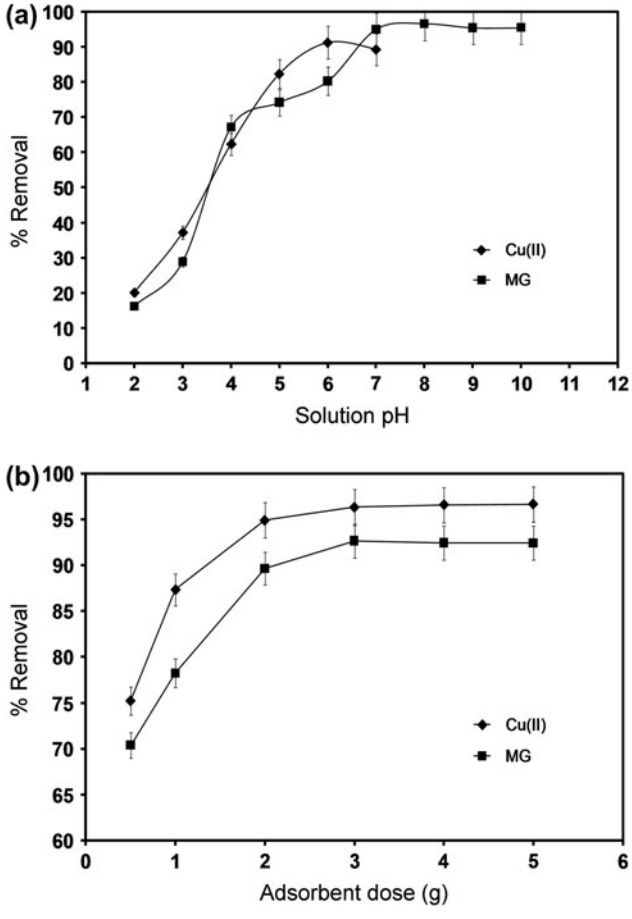

Fig. 2. (a) Effect of pH on adsorption of Cu(II) and MG by CMWB (experimental conditions: $C_0 = 50\,mg\,L^{-1}$, $m = 3\,g/0.1\,L$, agitation speed = 150 rpm, $T = 303\,K \pm 1$, contact time: 6 h) (b) Effect of adsorbent dose on adsorption of Cu(II) and MG by CMWB (experimental conditions: $C_0 = 50\,mg\,L^{-1}$, $pH_{Cu(II)} = 6.00$, $pH_{MG} = 8.00$, agitation speed = 150 rpm, $T = 303\,K \pm 1$, contact time: 6 h).

3.2.3. Effect of temperature

Fig. 3(a) illustrates the effect of temperature on the adsorption of Cu(II) and MG by the thermochemically modified wheat bran. Temperature was clearly an important parameter that controlled the adsorption process. The removal efficiencies decrease with increasing temperature which may be due to weakening of the bonds between the adsorbate molecules and the binding sites of the adsorbent [1]. The observed trend in decreased removal efficiency with increasing temperature suggests that adsorption process of Cu(II) and MG by CMWB is kinetically controlled by an exothermic process. Similar results have been reported in literature for adsorption of Cu(II) by chemically modified orange peel [21] and MG by tamarind fruit shell [22].

3.2.4. Effect of initial adsorbate concentration

Batch adsorption experiments were also carried out to study the effect of different initial adsorbate concentration on the adsorption of Cu(II) and MG by CMWB. Data obtained from the experiments is presented in Fig. 3(b). The experimental data indicate that the amount of adsorbate adsorbed per unit mass of the adsorbent increase with increase in initial adsorbate concentration from 20 to 100 $mg\,L^{-1}$. This behavior is a result of the increase in the driving force from the concentration gradient [1]. Also at higher adsorbate concentrations, the active sites of the adsorbent are surrounded by more adsorbate ions, and the adsorption phenomenon occurs more efficiently. So the value of q_e increases with the increase of initial adsorbate concentration [23]. Similar results were previously reported for adsorption of Cu(II) by *Hevea*

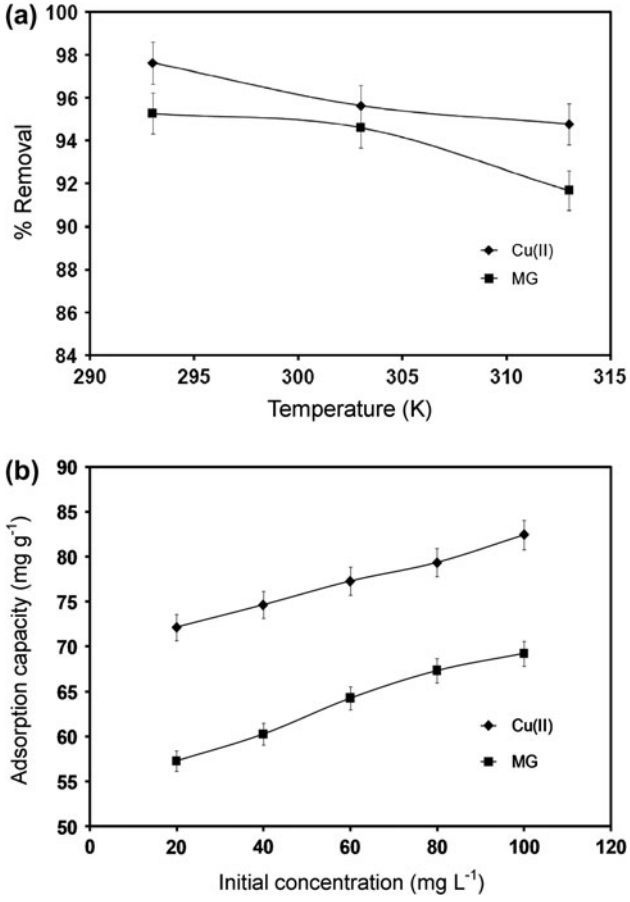

Fig. 3. (a) Effect of temperature on adsorption of Cu(II) and MG by CMWB (experimental conditions: $C_0 = 50$ mg L^{-1}, $pH_{Cu(II)} = 6.00$, $pH_{MG} = 8.00$, $m = 3\,g/0.1\,L$, agitation speed = 150 rpm, contact time: 6 h) (b) Effect of initial adsorbate concentration on adsorption of Cu(II) and MG by CMWB (experimental conditions: $pH_{Cu(II)} = 6.00$, $pH_{MG} = 8.00$, $m = 3\,g/0.1\,L$, agitation speed = 150 rpm, $T = 303\,K \pm 1$, contact time: 6 h).

brasiliensis leaf powder [24] and MG by *Ananus comosus* leaf powder [25].

3.3. Adsorption isotherms

The equilibrium sorption isotherm is fundamental in describing the interactive behavior between the adsorbate and the adsorbent and is important in the design and analysis of sorption systems. Adsorption equilibrium data are widely evaluated by different isotherm models. In the present investigation, the Freundlich, Langmuir, and D–R isotherm models were used to describe the equilibrium adsorption data [2].

$$\text{Langmuir: } \frac{C_e}{q_e} = \frac{C_e}{q_m} + \frac{1}{K_L q_m} \quad (3)$$

$$\text{Freundlich: } \log q_e = \log K_F + \left(\frac{1}{n}\right) \log C_e \quad (4)$$

$$\text{Dubinin–Radushkevich(D–R): } \ln q_e = \ln q_m - \beta\varepsilon^2 \quad (5)$$

The parameters and correlation coefficients obtained from the plots of Freundlich ($\log q_e$ vs. $\log C_e$), Langmuir (C_e/q_e vs. C_e), and D–R ($\ln q_e$ vs. ε^2) are listed in Table 2. For Cu(II)–CMWB system, the correlation coefficient values (R^2) at different temperatures were < 0.95, indicating that the equilibrium data did not fit the Langmuir model. The correlation coefficients at different temperatures were considerably high ($R^2 > 0.99$) for the Freundlich isotherm, which suggests that the system followed the Freundlich model. The applicability of the Freundlich isotherm for the mathematical description of the relationship between the amount of Cu(II) adsorbed and its equilibrium concentration in the solution implies that adsorption of Cu(II) by CMWB was multilayer adsorption applicable to heterogeneous surfaces. In contrast to Cu(II)–CMWB system, the equilibrium adsorption data of MG–CMWB system show a better correlation for the Langmuir than the Freundlich isotherm model, which indicates that MG is adsorbed onto the surface of CMWB forming a monolayer. The maximum monolayer adsorption capacity of CMWB for MG was calculated to be 67.54 mg g^{-1}.

In the Freundlich constant, n is an empirical parameter that varies with the degree of heterogeneity and is related to the distribution of bonded ions on the sorbent surface. In general, $n > 1$ illustrates that adsorbate is favorably adsorbed on an adsorbent, and the higher the n value the stronger the adsorption intensity. In particular, the value of n is significantly higher than unity at all the temperatures studied for both the systems.

The applicability of D–R isotherm model on the equilibrium adsorption data of Cu(II) and MG was also tested. The very low correlation coefficient values ($R^2 < 0.90$) for adsorption of both Cu(II) and MG by CMWB suggests that this model was not appropriate for describing the equilibrium adsorption data of Cu (II) and MG. The D–R model constant β, however, gives an idea about the mean free energy of adsorption (E) which in turn gives information about the nature of the adsorption process. The value of E is computed using the relation [1]:

$$E = \frac{1}{\sqrt{2\beta}} \quad (6)$$

Table 2
Isotherm constants for adsorption of Cu(II) and MG by CMWB

Adsorbate	T (K)	Langmuir			Freundlich			D–R			
		q_m (mg g^{-1})	K_L (L mg^{-1})	R^2	K_F (mg g^{-1}) (L mg^{-1})$^{1/n}$	n	R^2	q_m (mg g^{-1})	β (mmol^2 J^{-2})	E (kJ mol^{-1})	R^2
Cu(II)	293	73.159	1.431	0.948	17.367	7.562	0.998	55.681	2.029×10^{-9}	15.732	0.895
	303	71.922	1.094	0.945	15.984	6.988	0.991	52.193	2.352×10^{-9}	14.586	0.898
	313	70.072	0.936	0.949	14.083	6.217	0.994	50.462	2.816×10^{-9}	13.339	0.892
MG	293	67.547	1.208	0.995	12.685	6.791	0.967	42.079	2.551×10^{-9}	14.002	0.891
	303	64.781	0.962	0.999	10.499	6.085	0.962	39.911	2.874×10^{-9}	13.199	0.896
	313	61.165	0.877	0.997	8.821	5.678	0.966	37.268	3.197×10^{-9}	12.519	0.887

The magnitude of E may characterize the type of the adsorption as chemical ion exchange ($E = 8-16$ kJ mol^{-1}), or physical sorption ($E < 8$ kJ mol^{-1}) [1]. The mean free energy of adsorption for the present study was found to be > 8 kJ mol^{-1} at different temperatures for both the contaminants (Table 2) implying that the ongoing adsorption processes involve chemical adsorption.

3.4. Adsorption kinetics

The pseudo-first-order and pseudo-second-order kinetic models were used to study the adsorption kinetics of Cu(II) and MG onto CMWB [26].

$$\text{Pseudo-first-order: } \log(q_e - q_t) = \log q_e - \frac{k_1}{2.303}t \tag{7}$$

$$\text{Pseudo-second-order: } \frac{t}{q_t} = \frac{1}{k_2 q_e^2} + \frac{1}{q_e}t \tag{8}$$

The values of pseudo-first-order rate constants, k_1 and q_e were calculated from the slope and intercept of the plots of $\log(q_e - q_t)$ vs. t. The k_1 values, the correlation coefficients, and theoretical and experimental equilibrium adsorption capacity q_e for both the adsorbates are listed in Table 3. The low correlation coefficient values at all temperatures for both Cu(II) and MG suggest that the pseudo-first-order kinetic model is not suitable for describing the kinetics of the adsorption processes. Also, the theoretical and experimental equilibrium adsorption capacities (q_e) differ widely for both Cu(II) and MG, confirming that adsorption of Cu(II) and MB onto CMWB does not follow pseudo-first-order kinetics. On the other hand, the pseudo-second-order kinetic model shows excellent fit to the experimental adsorption kinetic data of Cu(II) and MB by CMWB at all temperatures studied. The pseudo-second-order rate constants, k_2 and q_e for adsorption of Cu(II) and MG at different temperatures as calculated from the plots of t/q_t vs. t and the corresponding correlation coefficients values are given in Table 3. All the correlation coefficients at different temperatures for both the adsorbate are considerably high ($R^2 > 0.99$). In addition the theoretical q_e values show good agreement with the experimental q_e values for both Cu(II) and MG, confirming that the ongoing adsorption processes proceed via a pseudo-second-order mechanism involving sharing or exchange of electrons between the adsorbate ions and the adsorbent.

In a well-agitated batch adsorption system, there is a possibility of intraparticle pore diffusion of adsorbate ions, which can be the rate-limiting step. Therefore, the possibility of intraparticle diffusion resistance affecting the adsorption process was explored by using the intraparticle diffusion model [26].

$$\text{Intraparticle diffusion: } q_t = k_i t^{0.5} \tag{9}$$

According to Eq. (8), if a plot of q_t vs. $t^{0.5}$ is linear and passes through the origin, then intraparticle diffusion is the sole rate-limiting step. In the present study, the plots of q_t vs. $t^{0.5}$ were linear at all temperatures for Cu(II) as well as MG, but the plots did not pass through the origin, implying that although intraparticle diffusion is involved in the adsorption processes, but it is not the sole rate-controlling step and that some other mechanisms also play an important role.

3.5. Activation energy and thermodynamic parameters

The activation energy E_a of the adsorption processes was calculated by the Arrhenius equation [27]:

Table 3
Kinetic parameters for adsorption of Cu(II) and MG by CMWB

Adsorbate	T (K)	$q_{e,\exp}$ (mg g^{-1})	Pseudo-first-order			Pseudo-second-order		
			$q_{e,\mathrm{cal}}$ (mg g^{-1})	k_1 (min^{-1})	R^2	$q_{e,\mathrm{cal}}$ (mg g^{-1})	k_2 (g mg^{-1} min^{-1})	R^2
Cu(II)	293	77.732	58.279	6.021×10^{-2}	0.924	78.178	7.342×10^{-4}	0.999
	303	75.133	56.881	3.283×10^{-2}	0.917	76.016	4.756×10^{-4}	0.996
	313	73.851	55.642	1.945×10^{-2}	0.932	74.641	1.861×10^{-4}	0.998
MG	293	63.358	47.118	9.150×10^{-2}	0.906	63.587	7.997×10^{-4}	0.999
	303	62.176	45.093	8.479×10^{-2}	0.913	62.992	4.962×10^{-4}	0.997
	313	60.923	43.789	6.388×10^{-2}	0.911	61.623	2.518×10^{-4}	0.999

$$\ln k = \ln A - \frac{E_a}{RT} \tag{10}$$

E_a was determined from the slope of the plots of $\ln k_2$ vs. $1/T$ and was calculated as 52.61 kJ mol^{-1} for Cu(II) and 44.38 kJ mol^{-1} for MG. The magnitude of activation energy gives an idea about the type of adsorption which is mainly physical or chemical. Low activation energies (<40 kJ mol^{-1}) are characteristic of physical adsorption process, while higher activation energies (>40 kJ mol^{-1}) suggest chemical adsorption [27]. Thus, it can be rightly said that adsorption of both Cu(II) and MG onto CMWB proceeds via a chemical-ion exchange mechanism.

Thermodynamic parameters, namely Gibbs free energy change (ΔG^0), enthalpy (ΔH^0), and entropy (ΔS^0) were calculated using the following equations for the temperature range 293–313 K [27]:

$$\Delta G^0 = -RT \ln K_C \tag{11}$$

$$K_C = \frac{C_a}{C_e} \tag{12}$$

$$\Delta G^0 = \Delta H^0 - T\Delta S^0 \tag{13}$$

The values of ΔG^0 were calculated as (−8.96, −7.36, and −5.29) kJ mol^{-1} for Cu(II) and (−6.26, −5.38, and −4.32) kJ mol^{-1} for MG at T = (293, 303, and 313 K), respectively. Negative values of ΔG^0 indicate the thermodynamically feasible and spontaneous nature of the adsorption processes. The values of ΔH^0 and ΔS^0 were determined from the slope and intercept of the plots of ΔG^0 vs. T (Fig. 4). Negative values of ΔH^0, −62.79 and −34.68 kJ mol^{-1} for Cu(II) and MG respectively, imply that the adsorption phenomenona are exothermic. In addition, negative ΔS^0 values for both Cu(II)-CMWB (−183.41 J mol^{-1}) and MG-CMWB (−96.13 J mol^{-1}) systems suggest that the adsorption processes are enthalpy driven.

3.6. Comparison of CMWB with other adsorbents

A comparative study of the Cu(II)/MG adsorption capacity of CMWB has been carried out with other reported adsorbents and is presented in Table 4. The capacity given for Cu(II) is not the $q_{\max}$, as it does not follow Langmuir model. This was calculated from the data obtained during batch experiments. From Table 4, it is evident that the maximum adsorption capacity of CMWB for Cu(II) and MG is comparable and moderately higher than that of many corresponding sorbent materials. Differences in the uptake capacity are due to the properties of each sorbent material such as structure, functional groups, and surface area. The easy availability and low preparation cost are some additional advantages, suggesting CMWB to be a better adsorbent for treatment of industrial effluents.

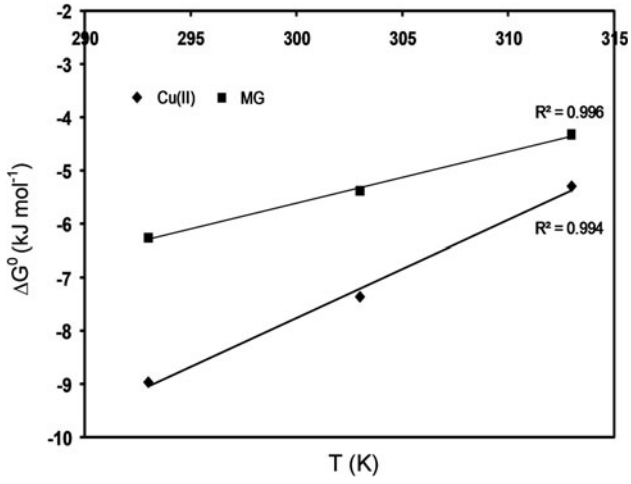

Fig. 4. Plot of Gibbs free energy change vs. temperature for adsorption of Cu(II) and MG by CMWB.

Table 4
Comparison of Cu(II) and MG adsorption capacity of CMWB with other reported low-cost adsorbents

Sorbent	Adsorption capacity ($mg\,g^{-1}$)	Reference
Cu(II)		
Cinnamomum camphora leaves powder	17.87	[28]
NaOH-pretreated *Marrubium globosum* ssp. *globosum* leaves powder	16.23	[29]
Pecan nutshell	85.90	[30]
Tea waste	48.00	[31]
Lentil shell	9.59	[32]
Wheat shell	17.42	[32]
Rice shell	2.95	[32]
Groundnut shell	7.60	[33]
Hazelnut shell activated carbon	58.27	[34]
Rose waste biomass	55.79	[35]
Pre-treated arca shell biomass	26.88	[36]
Tamarindus indica seed powder	133.24	[14]
CMWB	77.73	This study
MG		
Arundo donax root carbon	8.69	[37]
Waste apricot	116.27	[38]
Bentonite	7.72	[39]
Sugarcane dust	4.88	[40]
Degreased coffee bean	55.3	[41]
Sea shell powder	42.33	[1]
Hen feathers	26.1	[42]
Iron humate	19.2	[43]
Rubber wood sawdust	36.45	[44]
Maize cob powder	37.037	[45]
Lemon peel	51.73	[46]
Rattan sawdust	62.7	[47]
Ricinus communis based activated carbon	27.78	[48]
Pineapple leaf powder	54.64	[25]
CMWB	67.54	This study

4. Conclusion

Wheat bran can be readily modified with citric acid by a simple thermochemical procedure to develop a cationic adsorbent. FTIR analysis confirmed the introduction of free carboxylic acid groups during the treatment process. Increased surface area and larger pore size as inferred from the BET studies suggests that CMWB possess greater adsorption capacity than NWB. Operational parameters, such as solution pH, adsorbent dose, initial adsorbate concentration as well as temperature, greatly influenced the adsorption efficiency of CMWB. The adsorption equilibrium data was analyzed using the Langmuir, Freundlich, and D–R isotherm models. Cu(II)–CMWB system followed Freundlich model whereas MG–CMWB system followed Langmuir model. Pseudo-second-order model was found to describe the kinetics of the adsorption processes. Intraparticle diffusion model was not the sole rate-limiting step. The ΔG^0 values showed spontaneous and feasible nature of the adsorption processes. The adsorptions were also exothermic in nature. The comparison of adsorption efficiency of CMWB for Cu(II) and MG with a number of other reported adsorbents indicates its effectiveness for wastewater treatment. Both wheat bran and citric acid are easily available, cost effective and, biodegradable, and the modification process is simple. Therefore, the present strategy of improving the sorption property of wheat bran can be adopted to help increase its utility for contaminated water treatment.

Nomenclature

A	Arrhenius constant
C_a	equilibrium adsorbate concentration on the adsorbent ($mg\,L^{-1}$)
C_e	equilibrium adsorbate concentration in solution ($mg\,L^{-1}$)
C_i	initial adsorbate concentration ($mg\,L^{-1}$)
E	mean free energy ($kJ\,mol^{-1}$)
E_a	activation energy ($kJ\,mol^{-1}$)
ΔG^0	Gibbs free energy change ($kJ\,mol^{-1}$)
ΔH^0	enthalpy of reaction ($kJ\,mol^{-1}$)
I	intraparticle diffusion model constant
K_C	distribution coefficient for adsorption
K_F	Freundlich constant ($mg\,g^{-1}$) $(L\,g^{-1})^{1/n}$
K_L	Langmuir constant ($L\,mg^{-1}$)
k	rate constant
k_i	intraparticle diffusion rate constant ($mg\,g^{-1}\,min^{-0.5}$)
k_1	pseudo-first-order rate constant (min^{-1})
k_2	pseudo-second-order rate constant ($g\,mg^{-1}\,min^{-1}$)
m	mass of adsorbent (g)
n	Freundlich adsorption isotherm constant
q_e	equilibrium adsorbate concentration on adsorbent ($mg\,g^{-1}$)
q_m	maximum adsorption capacity ($mg\,g^{-1}$)
q_t	amount of adsorbate adsorbed at time t ($mg\,g^{-1}$)
R	universal gas constant ($8.314\ J\,mol^{-1}\,K^{-1}$)
R^2	correlation coefficient
ΔS^0	entropy of reaction ($J\,mol^{-1}\,K^{-1}$)

T temperature (K)
V volume of the solution (L)
β D–R isotherm constant ($mmol^2 J^{-2}$)
ε Polanyi potential ($J\,mmol^{-1}$) = $RT\ln(1 + 1/C_e)$

References

[1] S. Chowdhury, P. Saha, Sea shell powder as a new adsorbent to remove basic green 4 (malachite green) from aqueous solutions: Equilibrium, kinetic and thermodynamic studies, Chem. Eng. J. 164 (2010) 168–177.
[2] S. Chakraborty, S. Chowdhury, P.D. Saha, Adsorption of crystal violet from aqueous solution onto NaOH-modified rice husk, Carbohydr. Polym. 88 (2011) 1533–1541.
[3] A. Srinivasan, T. Viraraghavan, Decolorization of dye wastewaters by biosorbents: A review, J. Environ. Manage. 91 (2010) 1915–1929.
[4] Z. Aksu, Application of biosorption for the removal of organic pollutants: A review, Process Biochem. 40 (2005) 997–1026.
[5] T.A. Kurniawan, G.Y.S. Chan, W.-H. Lo, S. Babel, Comparisons of low-cost adsorbents for treating wastewaters laden with heavy metals, Sci. Total Environ. 366 (2006) 409–426.
[6] J.M. Awika, Major cereal grains production and use around the world, in: J.M. Awika, V. Piironen, S. Bean (Eds.), Advances in Cereal Science: Implications to Food Processing and Health Promotion, American Chemical Society, Northamptonshire, 2011, pp. 1–13.
[7] Y. Zhang, L. Pitkanen, J. Douglade, M. Tenkanen, C. Remond, C. Joly, Wheat bran arabinoxylans: Chemical structure and film properties of three isolated fractions, Carbohydr. Polym. 86 (2011) 852–859.
[8] X. Xie, S.W. Cui, W. Li, R. Tsao, Isolation and characterization of wheat bran starch, Food Res. Int. 41 (2008) 882–887.
[9] X. Sun, Z. Liu, Y. Qu, X. Li, The effects of wheat bran composition on the production of biomass-hydrolyzing enzymes by *Penicillium decumbens*, Appl. Biochem. Biotechnol. 146 (2008) 119–128.
[10] L. Prisenžňáková, G. Nosáľová, Z. Hromádková, A. Ebringerová, The pharmacological activity of wheat bran polysaccharides, Fitoterapia 81 (2010) 1037–1044.
[11] B. Zhu, T. Fan, D. Zhang, Adsorption of copper ions from aqueous solution by citric acid modified soybean straw, J. Hazard. Mater. 152 (2008) 300–308.
[12] J.D. McSweeny, R.M. Rowell, S.H. Min, Effect of citric acid modification of aspen wood on sorption of copper ion, J. Nat. Fibers 3 (2006) 43–58.
[13] T. Vaughan, C.W. Seo, W.E. Marshall, Removal of selected metal ions from aqueous solution using modified corncobs, Bioresour. Technol. 78 (2001) 133–139.
[14] S. Chowdhury, P.D. Saha, Biosorption kinetics, thermodynamics and isosteric heat of sorption of Cu(II) onto *Tamarindus indica* seed powder, Colloids Surf. B 88 (2011) 697–705.
[15] A. Ozer, D. Ozer, A. Ozer, The adsorption of copper(II) ions on to dehydrated wheat bran (DWB): Determination of the equilibrium and thermodynamic parameters, Process Biochem. 39 (2004) 2183–2191.
[16] Z.-Y. Yao, J.-H. Qi, L.-H. Wang, Equilibrium, kinetic and thermodynamic studies on the biosorption of Cu(II) onto chestnut shell, J. Hazard. Mater. 174 (2010) 137–143.
[17] R. Ahmad, R. Kumar, Adsorption studies of hazardous malachite green onto treated ginger waste, J. Environ. Manage. 91 (2010) 1032–1038.
[18] U. Farooq, M.A. Khan, M. Athar, J.A. Kozinski, Effect of modification of environmentally friendly biosorbent wheat (*Triticum aestivum*) on the biosorptive removal of cadmium(II) ions from aqueous solution, Chem. Eng. J. 171 (2011) 400–410.
[19] N. Nasuha, B.H. Hameed, A.T.M. Din, Rejected tea as a potential low cost adsorbent for the removal of methylene blue, J. Hazard. Mater. 175 (2010) 126–132.
[20] A. Ozcan, A.S. Ozcan, S. Tunali, T. Akar, I. Kiran, Determination of the equilibrium, kinetic and thermodynamic parameters of adsorption of copper(II) ions onto seeds of *Capsicum annuum*, J. Hazard. Mater. 124 (2005) 200–208.
[21] N.-C. Feng, X.-Y. Guo, S. Liang, Kinetic and thermodynamic studies on biosorption of Cu(II) by chemically modified orange peel, T. Nonferr. Metal Soc. 19 (2009) 1365–1370.
[22] P. Saha, S. Chowdhury, S. Gupta, I. Kumar, R. Kumar, Assessment on the removal of malachite green using tamarind fruit shell as biosorbent, Clean Soil Air Water 38 (2010) 437–445.
[23] R. Han, J. Zhang, P. Han, Y. Wang, Z. Zhao, M. Tang, Study of equilibrium, kinetic and thermodynamic parameters about methylene blue adsorption onto natural zeolite, Chem. Eng. J. 145 (2009) 496–504.
[24] W.S.W. Ngah, M.A.K.M. Hanafiah, Adsorption of copper on rubber (*Hevea brasiliensis*) leaf powder: Kinetic, equilibrium and thermodynamics studies, Biochem. Eng. J. 39 (2008) 521–530.
[25] S. Chowdhury, S. Chakraborty, P.D. Saha, Biosorption of basic green 4 from aqueous solution by *Ananus comosus* (pineapple) leaf powder, Colloids Surf. B 84 (2011) 520–527.
[26] P. Saha, S. Chowdhury, S. Gupta, I. Kumar, Insight into adsorption equilibrium, kinetics and thermodynamics of malachite green onto clayey soil of Indian origin, Chem. Eng. J. 165 (2010) 874–882.
[27] T.S. Anirudhan, P.G. Radhakrishnan, Thermodynamics and kinetics of adsorption of Cu (II) from aqueous solution onto a new cation exchanger derived from tamarind fruit shell, J. Chem. Thermodyn. 40 (2008) 702–709.
[28] H. Chen, G. Dai, J. Zhao, A. Zhong, J. Wu, H. Yan, Removal of copper(II) ions by a biosorbent—*Cinnamomum camphora* leaves powder, J. Hazard. Mater. 177 (2010) 228–236.
[29] M. Kilic, H. Yazıcı, M. Solak, A comprehensive study on removal and recovery of copper(II) from aqueous solutions by NaOH-pretreated *Marrubium globosum* ssp. globosum leaves powder: Potential for utilizing the copper(II) condensed desorption solutions in agricultural applications, Bioresour. Technol. 100 (2009) 2130–2137.
[30] J.C.P. Vaghetti, E.C. Lima, B. Royer, B.M. da Cunha, N.F. Cardoso, J.L. Brasil, S.L.P. Dias, Pecan nutshell as biosorbent to remove Cu(II), Mn(II) and Pb(II) from aqueous solutions, J. Hazard. Mater. 162 (2009) 270–280.
[31] B.M.W.P.K. Amarasinghe, R.A. Williams, Tea waste as a low cost adsorbent for the removal of Cu and Pb from wastewater, Chem. Eng. J. 132 (2007) 299–309.
[32] H. Aydin, Y. Bulut, C. Yerlikaya, Removal of copper (II) from aqueous solution by adsorption onto low-cost adsorbents, J. Environ. Manage. 87 (2008) 37–45.
[33] S.R. Shukla, R.S. Pai, Adsorption of Cu(II), Ni(II) and Zn(II) on dye loaded groundnut shells and sawdust, Sep. Purif. Technol. 43 (2005) 1–8.
[34] E. Demirbas, N. Dizge, M.T. Sulak, M. Kobya, Adsorption kinetics and equilibrium of copper from aqueous solutions using hazelnut shell activated carbon, Chem. Eng. J. 148 (2009) 480–487.
[35] A.R. Iftikhara, H.N. Bhattia, M.A. Hanif, R. Nadeem, Kinetic and thermodynamic aspects of Cu(II) and Cr(III) removal from aqueous solutions using rose waste biomass, J. Hazard. Mater. 161 (2009) 941–947.
[36] S. Dahiya, R.M. Tripathi, A.G. Hegde, Biosorption of heavy metals and radionuclide from aqueous solutions by pre-treated arca shell biomass, J. Hazard. Mater. 150 (2008) 376–386.
[37] J. Zhang, Y. Li, C. Zhang, Y. Jing, Adsorption of malachite green from aqueous solution onto carbon prepared from *Arundo donax* root, J. Hazard. Mater. 150 (2008) 774–782.

[38] C.A. Basar, Applicability of the various adsorption models of three dyes adsorption onto activated carbon prepared from waste apricot, J. Hazard. Mater. 135 (2006) 232–241.
[39] S.S. Tahir, N. Rauf, Removal of a cationic dye from aqueous solutions by adsorption onto bentonite clay, Chemosphere 63 (2006) 1842–1848.
[40] S.D. Khattri, M.K. Singh, Colour removal from dye wastewater using sugar cane dust as an adsorbent, Adsorpt. Sci. Technol. 17 (1999) 269–282.
[41] M.-H. Baek, C.O. Ijagbemi, O. Se-Jin, D.-S. Kim, Removal of malachite green from aqueous solution using degreased coffee bean, J. Hazard. Mater. 176 (2010) 820–828.
[42] A. Mittal, Adsorption kinetics of removal of a toxic dye, malachite green, from wastewater by using hen feathers, J. Hazard. Mater. 133 (2006) 196–202.
[43] P. Janos, Sorption of basic dyes onto iron humate, Environ. Sci. Technol. 37 (2003) 5792–5798.
[44] K.V. Kumar, S. Sivanesan, Isotherms for malachite green onto rubber wood (*Hevea brasiliensis*) sawdust: Comparison of linear and non-linear methods, Dyes Pigm. 72 (2007) 124–129.
[45] G.H. Sonawane, V.S. Shrivastava, Kinetics of decolourization of malachite green from aqueous medium by maize cob (*Zea maize*): An agricultural solid waste, Desalination 247 (2009) 430–441.
[46] K.V. Kumar, Optimum sorption isotherm by linear and non-linear methods for malachite green onto lemon peel, Dyes Pigm. 74 (2007) 595–597.
[47] B.H. Hameed, M.I. El-Khaiary, Malachite green adsorption by rattan sawdust: Isotherm, kinetic and mechanism modelling, J. Hazard. Mater. 159 (2008) 574–579.
[48] T. Santhi, S. Manonmani, T. Smitha, Removal of malachite green from aqueous solution by activated carbon prepared from the epicarp of *Ricinus communis* by adsorption, J. Hazard. Mater. 179 (2010) 178–186.